

Microwave Spectrum, Conformation and Intramolecular Hydrogen Bonding of 2,2,2-Trifluoroethanethiol (CF₃CH₂SH)

Harald Møllendal[†]

Centre for Theoretical and Computational Chemistry (CTCC), Department of Chemistry, University of Oslo, Post Office Box 1033 Blindern, NO-0315, Oslo Norway

Received: April 22, 2008; Revised Manuscript Received: May 26, 2008

The microwave spectrum of 2,2,2-trifluoroethanethiol, CF₃CH₂SH, and of one deuterated species, CF₃CH₂SD, has been investigated in the 7–80 GHz spectral interval. The microwave spectra of the ground and three vibrationally excited states belonging to three different normal modes of one conformer were assigned for the parent species, and the vibrational frequencies of these fundamentals were determined by relative intensity measurements. Only the ground vibrational state was assigned for the deuterated species. The identified form has a *synclinal* arrangement for the H–S–C–C chain of atoms and the corresponding dihedral angle is 68(5)° from *synperiplanar* (0°). A weak intramolecular hydrogen bond formed between the thiol (SH) group and one of the fluorine atoms is stabilizing this conformer. There is no evidence in the microwave spectrum for the H–S–C–C *antiperiplanar* form. The hydrogen atom of the thiol group should have the ability to tunnel between two equivalent *synclinal* potential wells, but no splittings of spectral lines due to tunneling were observed. The microwave work was augmented by quantum chemical calculations at the B3LYP/aug-cc-pVTZ and MP2/aug-cc-pVTZ levels of theory.

Introduction

Intramolecular hydrogen (H) bonding has interested this laboratory for years.¹ The thiol (SH) group is an interesting weak proton donor capable of forming internal H bonds with a variety of acceptor atoms or groups. π electrons are, for example, acceptors in one of the assigned rotameric forms of propargylthiol (HSCH₂C≡CH),^{2,3} 2-propenethiol (H₂C=CHCH₂SH),⁴ 3-mercaptopropionitrile (HSCH₂CH₂C≡N),⁵ 3-butene-1-thiol (HSCH₂CH₂CH=CH₂),^{6,7} 3-butyne-1-thiol (HSCH₂CH₂C≡CH),⁸ (Z)-3-mercapto-2-propenenitrile (HSCH=CHC≡N),⁹ and 2-furanmethanethiol (C₄H₃OCH₂SH).¹⁰ Pseudo- π electrons¹¹ are acceptor in the assigned conformer of cyclopropanemethanethiol (C₃H₅CH₂SH)¹² and in two rotamers of thiiranemethanethiol (C₂H₃SCH₂SH).¹³ An oxygen atom acts as acceptor in one of the rotamers of C₄H₃OCH₂SH,¹⁰ and in the identified form of methylthioglycolate (HSCH₂COCH₃),¹⁴ whereas a nitrogen atom is acceptor in one of the conformers assigned for aminoethanethiol (H₂NCH₂CH₂SH).^{15–17} In one rotamer of thiiranemethanethiol (C₂H₃SCH₂SH)¹³ and one rotamer of 1,2-ethanedithiol (HSCH₂CH₂SH),¹⁸ a sulfur atom acts as acceptor for the H atom of the thiol group.

2,2,2-Trifluoroethanethiol (CF₃CH₂SH) was chosen for the present study because the thiol group may form an internal H bond with one of the fluorine atoms. The S–H···F (dots indicate nonbonded interaction) type of intramolecular H bond has not previously been investigated by microwave (MW) spectroscopy.

Two rotameric forms, denoted *sc* and *ap* are possible for 2,2,2-trifluoroethanethiol. These forms are depicted in Figure 1, where the atom numbering is also given. The H7–S1–C2–C3 link of atoms is *synclinal* (obsolete “gauche”), roughly 60° from the *synperiplanar* (0°) conformation, in *sc*, and *anticlinal* (180°; obsolete “trans”) in *ap*. The H7 atom is brought into close

contact with one of the fluorine atoms (F4) in *sc*, forming an internal H bond.

Microwave (MW) spectroscopy was chosen as the experimental method for the investigation of CF₃CH₂SH and its isotopologue CF₃CH₂SD, because of its extreme accuracy and resolution, which is ideal for conformational studies. The MW investigation has been augmented by quantum chemical calculations performed at high levels of theory. The current calculations were conducted to obtain information for use in assigning the MW spectrum and investigating the properties of the potential-energy hypersurface.

Experimental Section

A commercial sample of 2,2,2-trifluoroethanethiol was purified by preparative gas chromatography before use. The spectrum was recorded in the 7–80 GHz frequency interval by Stark-modulation spectroscopy, using the microwave spectrometer of the University of Oslo, which measures the frequency of individual transitions with an estimated accuracy (three standard deviations) of ≈0.10 MHz. Details of the construction and operation of this spectrometer has been given elsewhere.^{19,20} Most of the spectra were recorded with the Stark cell cooled to about –50 °C with solid CO₂, in an attempt to increase the intensity. A few spectra were also taken at room temperature. The deuterated species, CF₃CH₂SD, was produced by mixing fumes of the parent species with fumes of heavy water in the cell of the spectrometer. Roughly 30% deuteration was achieved in this manner, according to rough relative intensity measurements.

Quantum-Chemical Calculations. The present ab initio and density functional theory (DFT) calculations were conducted employing the Gaussian 03 suite of programs,²¹ running on the 64 processor HP “superdome” computer in Oslo. Electron correlation was taken into consideration in the ab initio calculations using Møller–Plesset second-order perturbation calculations (MP2).²² Becke’s three-parameter hybrid func-

[†] Fax: +47 2285 5441. Tel: +47 2285 5674. E-mail: harald.mollendal@kjemi.uio.no

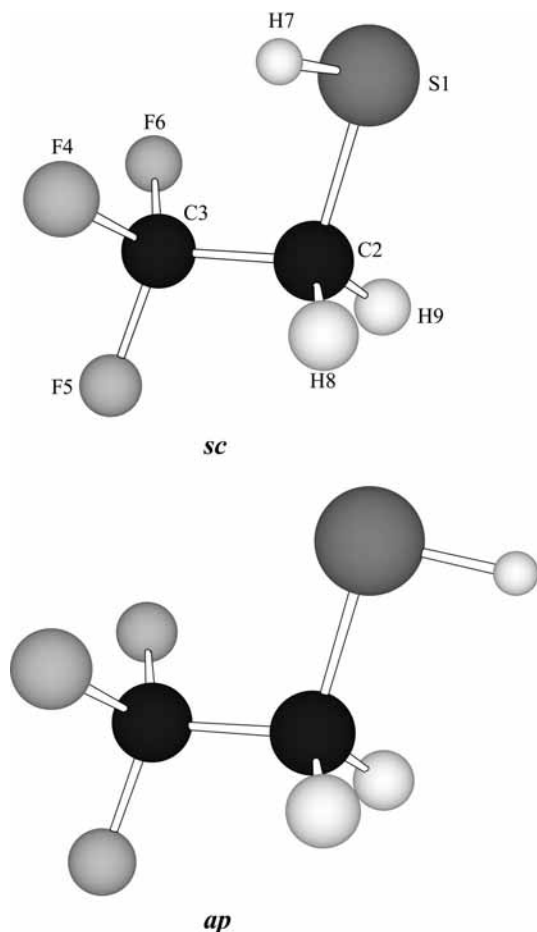


Figure 1. Models of two conformations of $\text{CF}_3\text{CH}_2\text{SH}$ with atom numbering. The H7-S1-C2-C3 dihedral angle is *synclinal* in the conformer denoted *sc*, and *antiperiplanar* in the *ap* rotamer. The MW spectrum of *sc* was assigned in this work and *ap* is found to be a transition state in the B3LYP calculations.

tional²³ employing the Lee, Yang and Parr correlation functional²⁴ (B3LYP) was employed in the DFT calculations. The aug-cc-pVTZ basis set,²⁵ which is of triple- ζ quality and includes polarization and diffuse functions, was used throughout the calculations. This relatively large basis set was chosen because it has been optimized for the atoms of the title compound.²⁵ The MP2 and B3LYP procedures were employed because it is our experience that they deal successfully with compounds similar to $\text{CF}_3\text{CH}_2\text{SH}$. The default convergence criteria of Gaussian 03 were employed.

Rotation about the C2-S1 bond (see Figure 1) may produce rotational isomerism in this compound. B3LYP calculations were performed first in an attempt to predict which rotameric forms are minima ("stable" conformers) of the potential-energy hypersurface. Calculations of energies were performed for the 0 to 180° interval in steps of 10° of the H7-S1-C2-C3 dihedral angle, employing the scan option of the Gaussian 03 program, allowing all remaining structural parameters to vary freely. The resulting potential function, which is shown in Figure 2, has only one minimum at about 70° for the H7-S1-C2-C3 dihedral angle, and two maxima at about 0 and 180° . These calculations therefore predict that there is only one "stable" form of $\text{CF}_3\text{CH}_2\text{SH}$, namely *sc*.

Separate B3LYP calculations of the structures, energies, dipole moments, vibrational frequencies, Watson's *S*-reduction centrifugal distortion constants,²⁶ and the vibration-rotation constants (the α 's)²⁷ were then performed for *sc*. The starting

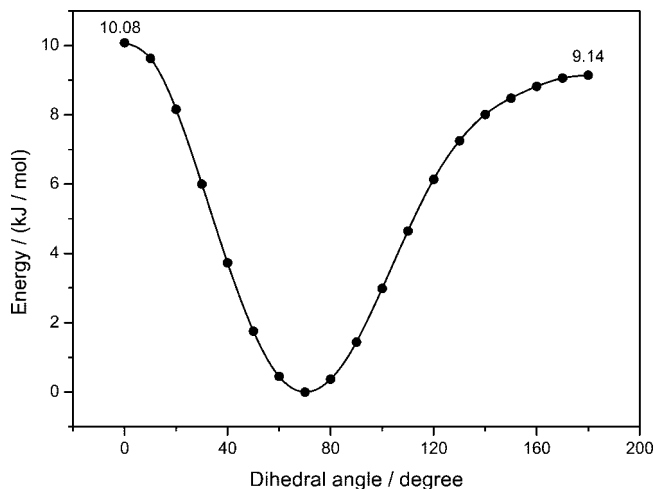


Figure 2. B3LYP/aug-cc-pVTZ potential function for torsion about the C2-S1 bond. Values of the H7-S1-C2-C3 dihedral angle are given on the abscissa. This function has a minimum at 70.2° from *synperiplanar* (0°), and two maxima at 0° (10.08 kJ/mol above the minimum) and at 180° (9.14 kJ/mol above the minimum).

values of the H7-S1-C2-C3 dihedral angles were chosen to be close to 70° , respectively. Full geometry optimizations with no symmetry restrictions were undertaken. The H7-S1-C2-C3 dihedral angle was found to be 70.2° for *sc* in these calculations. Only positive values were found for the harmonic vibrational frequencies of this conformer, as expected for a minimum on the potential-energy hypersurface. The B3LYP structure of *sc* is listed in Table 1 and parameters of spectroscopic interest are displayed in Tables 2 and 5 where experimental results are also included for convenient comparison with experiment. The harmonic vibrational frequencies are listed in Table 6S in the Supporting Information.

The two maxima of the potential function were explored next using the transition state option of Gaussian 03. The first transition state was found for a value of exactly 0° of the H7-S1-C2-C3 dihedral angle and an electronic energy that is 10.08 kJ/mol higher than the electronic energy of *sc*. The second transition state was found at 180° (9.16 kJ/mol above the energy of *sc*). Each of these maxima has one imaginary vibrational frequency associated with the torsion about the C2-S1 bond, which indicates that they are first-order transition states. The full potential function for rotation about the C2-S9 bond not corrected for zero-point energies could now be constructed, as shown in Figure 2.

MP2/aug-cc-pVTZ calculations of the structure of *sc*, its dipole moment components, harmonic vibrational frequencies and quartic centrifugal distortion constants were repeated, because we wanted to compare the results obtained by the B3LYP and MP2 methods with each other as well as with the experimental results. MP2 results are therefore included in Table 1 and 2, and the vibrational frequencies are given in Table 6S in the Supporting Information.

Comparison of the B3LYP and MP2 structures (Table 1) reveals rather minor differences. It is noted that the B3LYP S1-C2 bond length is 1.6 pm longer than the MP2 bond length, whereas the other bond lengths agree to within less than 1 pm. The bond angles are the same to within 1° . The dihedral angles associated with the thiol group differ by less than about 2° . The important H7-S1-C2-C3 dihedral angle is 68.5° in the MP2 calculations, compared to the B3LYP value of 70.2° .

Accurate experimental structures of related compounds are available for comparison with the theoretical structures in Table

TABLE 1: B3LYP^{a,b} and MP2 Structure^{a,c} of the *sc* Conformer of 2,2,2-Trifluoroethanethiol

	B3LYP	MP2
Distance (pm)		
S1–C2	182.3	180.7
S1–H7	134.5	133.7
C2–C3	151.5	150.9
C2–H8	108.7	108.7
C2–H9	108.8	108.8
C3–F4	134.9	134.4
C3–F5	135.3	134.7
C3–F6	134.2	133.7
Angle (deg)		
C2–S1–H7	96.6	95.8
S1–C2–C3	114.7	113.7
S1–C2–H8	111.0	111.4
S1–C2–H9	106.4	106.8
C3–C2–H8	108.2	108.2
C3–C2–H9	107.9	107.8
H8–C2–H9	108.4	108.8
C2–C3–F4	112.0	111.8
C2–C3–F5	109.8	109.9
C2–C3–F6	112.8	112.6
F4–C3–F5	107.0	107.2
F4–C3–F6	107.6	107.7
F5–C3–F6	107.2	107.4
Dihedral Angle (deg)		
H7–S1–C2–C3	70.2	68.5
H7–S1–C2–H8	–52.8	–54.1
H7–S1–C2–H9	–170.6	–172.7
S1–C2–C3–F4	–61.0	–60.7
S1–C2–C3–F5	–179.8	–179.6
S1–C2–C3–F6	60.6	60.7

^a Basis set: aug-cc-pVTZ.25 ^b Energy corrected for zero-point vibrational energies: –2037 087.5 kJ/mol. ^c Energy corrected for zero-point vibrational energies: –2034 088.1 kJ/mol.

TABLE 2: B3LYP^a and MP2^{a,b} Parameters of Spectroscopic Interest of the *sc* Conformer of CF₃CH₂SH

	B3LYP	MP2	experimental ^c
Rotational Constants (MHz)			
<i>A</i>	5205.0	5247.6	5252.22429(99)
<i>B</i>	1746.4	1784.7	1778.2900(37)
<i>C</i>	1736.1	1774.4	1767.5476(40)
Quartic Centrifugal Distortion Constants ^a (kHz)			
<i>D_J</i>	0.261	0.261	0.26247(13)
<i>D_{JK}</i>	2.43	2.21	2.3140(11)
<i>D_K</i>	–1.41	–1.20	–1.29260(60)
<i>d₁</i>	0.000402	0.000346	0.00346(44)
<i>d₂</i>	–0.000167	–0.000202	–0.054(20)
Dipole Moment ^d (10 ^{–30} C m)			
<i>μ_a</i>	3.2	3.3	
<i>μ_b</i>	3.9	4.2	
<i>μ_c</i>	3.4	3.7	
<i>μ_{tot}</i>	6.0	6.5	

^a Basis set: aug-cc-pVTZ. ^b S-reduction.²⁶ ^c Uncertainties represent one standard deviation. ^d 1 debye = 3.33564 × 10^{–30} C m.

1. The C–S *r*₀ bond length is 181.9(5) pm in CH₃SH,²⁸ whereas the *r_s* bond length is 182.0(5) pm in the H–S–C–C *anti-periplanar* conformer of CH₃CH₂SH,²⁹ and 181.4(9) pm in the *synclinal* form of this compound.³⁰ The S–H *r*₀ bond length is 133.6(10) pm in CH₃SH,²⁸ and the *r_s* bond length is 132.2(6) pm in *anti-periplanar* CH₃CH₂SH²⁹ and 133.6(10) in *synclinal* CH₃CH₂SH.³⁰ These values are close to the theoretical counterparts shown in Table 1.

TABLE 3: Spectroscopic Constants^a of the Ground Vibrational State of the *sc* Conformer of CF₃CH₂SH^b and CF₃CH₂SD^c

	CF ₃ CH ₂ SH	CF ₃ CH ₂ SD
<i>A</i> (MHz)	5252.22429(99)	5163.4907(29)
<i>B</i> (MHz)	1778.2900(37)	1751.6029(69)
<i>C</i> (MHz)	1767.5476(40)	1738.0204(74)
<i>D_J</i> (kHz)	0.26247(13)	0.2569(20)
<i>D_{JK}</i> (kHz)	2.3140(11)	2.1492(22)
<i>D_K</i> (kHz)	–1.29260(60)	–1.141(31)
<i>d₁</i> (kHz)	0.00346(44)	0.00346 ^d
<i>d₂</i> (kHz)	–0.054(20)	–0.054 ^d
<i>Φ_{JK}</i> ^e (Hz)	–0.00113(40)	<i>f</i>
rms ^g (MHz)	0.107	0.075
no. of transitions ^h	884	202

^a S-reduction *F*-representation. Uncertainties represent one standard deviation. ^b Spectrum in Table 1S in the Supporting Information. ^c Spectrum in Table 5S in the Supporting Information. ^d Fixed. ^e Further sextic centrifugal distortion constants preset at zero. ^f Not fitted. Preset at zero. ^g Root-mean-square deviation. ^h Number of transitions used in the least-squares fit.

TABLE 4: Spectroscopic Constants^a of Vibrationally Excited States of the *sc* Conformer of CF₃CH₂SH

	C–C torsion ^b	lowest bending ^c	C–S torsion ^d
<i>A</i> (MHz)	5243.8971(16)	5258.6331(14)	5253.7851(48)
<i>B</i> (MHz)	1775.809(12)	1777.0791(23)	1776.288(25)
<i>C</i> (MHz)	1766.840(12)	1765.4206(25)	1768.825(26)
<i>D_J</i> (kHz)	0.26099(30)	0.26120(26)	0.2760(20)
<i>D_{JK}</i> (kHz)	2.4335(16)	2.3213(12)	2.3200(47)
<i>D_K</i> (kHz)	–1.4428(45)	–1.1099(30)	–1.492(53)
<i>d₁</i> (kHz)	0.0115(58)	0.00346 ^e	0.00346 ^e
<i>d₂</i> (kHz)	0.26(12)	–0.054 ^e	–0.054 ^e
rms ^f (MHz)	0.100	0.075	0.149
no. of transitions ^g	425	202	93

^a S-reduction *F*-representation. Uncertainties represent one standard deviation. ^b Spectrum in Table 2S in the Supporting Information. ^c Spectrum in Table 3S in the Supporting Information. ^d Spectrum in Table 4S in the Supporting Information. ^e Fixed. ^f Root-mean-square deviation. ^g Number of transitions used in the least-squares fit.

The theoretical C2–C3 bond length is calculated to be rather short (151.5 (B3LYP) and 150.9 pm (MP2); Table 1). However, the C–C distance in CF₃CH₃ is even a bit shorter (*r_a* = 150.0(5) pm),³¹ whereas the C–F *r_a* bond length is 135.3(4), which is similar to the corresponding theoretical predictions in Table 1. The good overall agreement with the structures of related compounds for which accurate experimental values are available, is an indication that the predictions of Table 1 are indeed accurate.

Spectrum and Assignment. The quantum chemical calculations above indicate that only *sc*, which is a near-prolate rotor (Ray’s asymmetry parameter³² *κ* ≈ –0.99), exists for CF₃CH₂SH. All three dipole moment components of this rotamer are approximately 3 × 10^{–30} C m (Table 2). The rotational constants are comparatively small and there are five fundamental vibrational frequencies below 500 cm^{–1}, according to the present quantum chemical calculations (not given in Table 1 or 2). It was expected that all this would lead to a very dense spectrum with absorption lines occurring every few MHz throughout the entire spectral region, and this was indeed observed.

The *a*- and *b*-type transitions are expected to follow the ordinary rigid-rotor selection rules. However, *μ_c* is antisymmetrical with respect to the torsion of the thiol group and *c*-type rotational transitions therefore connect energy levels in torsional states of opposite parity and will depend strongly on the energy

TABLE 5: Vibration–Rotation Constants of the *sc* Conformer of CF₃CH₂SH

	C2–C3 torsion		lowest bending		S1–C2 torsion	
	ex ^a	theo ^a	ex ^a	theo ^b	ex ^a	theo ^b
α_A (MHz)	8.3271 (19)	8.16	-6.4088 (17)	-9.57	-1.5608 (49)	-1.73
α_B (MHz)	2.481 (13)	2.70	1.2109 (44)	0.58	2.002 (25)	2.42
α_C (MHz)	0.708 (13)	0.82	2.1270 (47)	2.30	-1.277 (26)	0.57

^a From experimental rotational constants with $\alpha_X = X_0 - X_1$, where X is a rotational constant; see text. ^b From the B3LYP calculations.

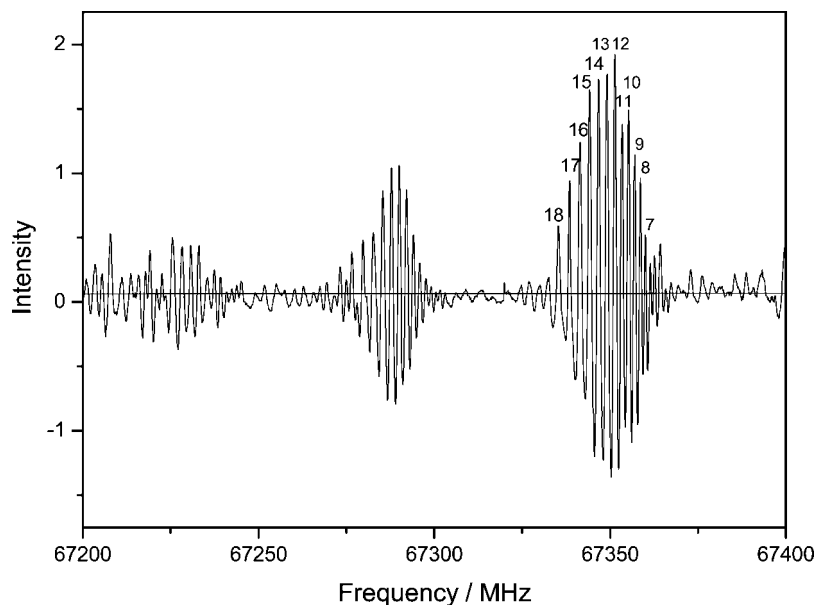


Figure 3. Spectrum of the *a*-type *R*-branch $J = 19 \leftarrow 18$ transitions taken at a Stark field strength of approximately 22 V/cm showing the ground (far right) and vibrationally excited states (middle and left). The values of the K_{-1} pseudo quantum numbers are indicated above several transitions of the ground vibrational state.

of the separation, Δ (the “tunneling frequency”), of these states. The selection rules of the *c*-type lines are therefore those of a rigid rotor plus (+) \leftarrow (−), or (−) \leftarrow (+), whereas the *a*- and *b*-type transitions occur between states of the same parity and will therefore depend little on Δ .

A prediction of Δ of *sc* is not given by the Gaussian program and a rough estimate of its value was therefore estimated as follows using the potential curve shown in Figure 2, which was fitted to the expression $V(\phi) = \sum 1/2V_i(1 - \cos(i\phi))$. Only the three first terms of this expansion were retained and they were found to be $V_1 = 296.5$, $V_2 = -668.7$ and $V_3 = -375.1$ cm⁻¹, respectively. Following Lewis et al.,³³ the energy levels, E , were calculated from $-B d^2\Psi/d\phi^2 + V(\phi) = E\Psi$, using a program by Bjørseth.³⁴ The value of B was calculated as described by Pitzer and Gwinn³⁵ to be 9.429 cm⁻¹ for CF₃CH₂SH, and 4.748 cm⁻¹ for CF₃CH₂SD. In this manner, Δ was estimated to be 15 MHz for the parent species and 0.2 MHz for the deuterated species. Similarly, the C2–S1 torsional frequency was estimated to be 201 cm⁻¹, compared to the B3LYP value of 219 cm⁻¹ (Table 6S; Supporting Information).

Interestingly, the MW spectrum of the alcohol analogue (CF₃CH₂OH) revealed that $\Delta = 5868.6952(16)$ MHz in this compound.³⁶ However, a large decrease in the tunneling frequency on going from alcohols to their thiol analogues seems to be the rule. For example, the tunneling frequency, which is 644319.69 MHz in HOCH₂C≡CH,³⁷ is reduced to 6895 MHz in HSCH₂C≡CH.^{3,38} In the *synclinal* conformer of CH₃CH₂OH it is 97734.3 MHz,³⁹ but in the similar rotamer of CH₃CH₂SH, a much smaller value of 1753.84(29) has been determined.³⁰ Similarly, the reduction of Δ from 46798.50(11) MHz in (CH₃)₂CHOH⁴⁰ to 562.4 MHz was seen in (CH₃)₂CHSH.⁴¹ The

tunneling frequency of 1.664(22) MHz in cyclopropanethiol, C₃H₅SH,⁴² is much smaller than 4115.26(42) MHz in the oxygen analogue cyclopropanol, C₃H₅OH.⁴³ A relatively small tunneling frequency was therefore expected for *sc*.

Two types of pileups of spectral lines were predicted for *sc* because it is nearly completely prolate ($\kappa \approx -0.99$) and has sizable dipole moment components along all three inertial axes (Table 2). The pileups associated with the ^a*R*-lines should be separated by almost exactly $B + C$, where B and C are rotational constants. The ^b*Q*-transitions should, on the other hand, have band heads at frequencies, ν , given by $\nu \approx [A - (B + C)/2](2K_{-1} + 1)$, where A , B , and C are the rotational constants and K_{-1} is the lower pseudo quantum number of these perpendicular transitions. Band heads similar to those of the ^b*Q*-transitions were also expected to occur at $\nu \approx [A - (B + C)/2](2K_{-1} + 1) \pm \Delta$ for the *c*-type *Q*-branch lines. Numerous *Q*-branch transitions associated with low and intermediate values of the principal quantum number J were expected to be seen near the *b*- and *c*-type band heads.

The high- K_{-1} *a*-type *R*-branch transitions are practically degenerate and are therefore modulated at very low Stark voltages. This simplifies this most complicated spectrum because the majority of transitions are suppressed at low Stark voltages. The pileup associated with the $J = 19 \leftarrow 18$ ^a*R*-transition shown in Figure 3 is typical. The coalescing K_{-1} -pairs having values between 7 and 18 are indicated on the ground vibrational state in this figure. The different K_{-1} -pairs are separated from each other owing to the effect of centrifugal distortion. This and other ^a*R*-pileups were used to get the first determination of the B and C rotational constants.

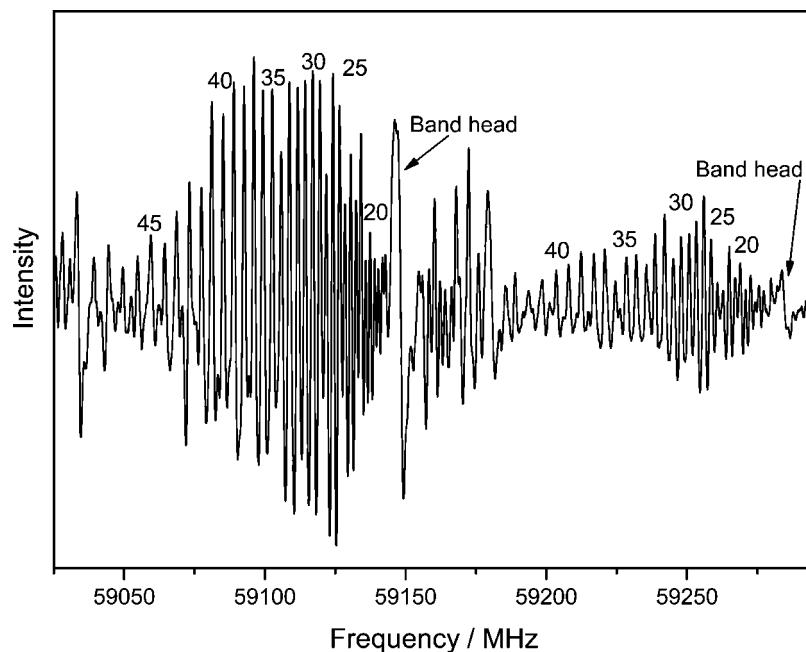


Figure 4. Band-head regions of the ground and first excited state of the lowest bending vibration of the bQ -branch $K_{-1} = 9 \leftarrow 8$ series. The band head of the ground vibrational state has a frequency of 59 148 MHz. The corresponding band head of the first excited state of the lowest bending vibration occurs at 59 284 MHz. The values of the J quantum number of selected lines are indicated above the lines. This spectrum was recorded using a Stark field strength of approximately 22 V/cm.

Different values of the B and C rotational constants of the (+)- and of the (-)-states would lead to splittings of the aR -lines. A large Δ normally results in noticeable differences between the rotational constants belonging to the (+)- and (-)-states. However, a resolution into lines belonging to these two states was not observed for a -type lines of the title compound and is presumably less than 0.5 MHz, which is the resolution of our spectrometer. This was the first experimental indication that the tunneling frequency, Δ , is indeed small in sc .

The spectroscopic constants in Table 2 predict that the low and intermediate- J b - and c -type Q -branch lines will coalesce into band heads, as noted above. However, separation between the transitions increases with increasing values of the J quantum number. Moreover, these transitions have rapid Stark effects. The band head region associated with the $K_{-1} = 9 \leftarrow 8$ transitions is displayed in Figure 4. The frequencies of the band heads were used to obtain the first estimate of all three rotational constants.

bR -branch transitions having $K_{-1} \geq 3$ consist of coalescing pairs, which have rapid Stark effects. The preliminary spectroscopic constants obtained as outlined above were used to predict the frequencies of transitions with $J < 10$, which were found close to their predicted frequencies. New transitions involving higher and higher values of J and $K_{-1} \geq 3$ were added successively and fitted with Sørensen's program Rotfit⁴⁴ to Watson's S -reduction Hamiltonian using the F -representation.²⁶ The maximum value of J being 77 and $K_{-1} = 33$. Finally, the bQ -branch lines with $K_{-1} \geq 3$ with a maximum of $J = 69$ were assigned and included in the fit. A total of 884 transitions were assigned in this manner. The spectrum is listed in Table 1S in the Supporting Information and the spectroscopic constants are displayed in Tables 2 and 3. The effect of centrifugal distortion is relatively small, as can be seen from Table 1S, and only the five quartic centrifugal distortion constants and one sextic constant, Φ_{JK} , were found to be sufficient to obtain a root-mean-square deviation, which is similar to the accuracy of the spectral measurements (± 0.10 MHz). The accuracy of D_J , D_{JK} , and D_K

is high (Tables 2 and 3), but low for d_1 and d_2 for this asymmetric top, whose $\kappa = -0.9938$ (Table 1S). The low accuracy of d_1 and d_2 was expected because the spectrum depends little on these constants, which become exactly zero for $\kappa = -1$. None of the b -type lines used in the fit were split, which is another indication that the tunneling frequency, Δ , is indeed small.

Attempts were made to include b -type lines with $K_{-1} < 2$, but it was frequently found that they do not fit well to this Hamiltonian but deviate in some cases by as much as a few megahertz. Inclusion of additional sextic centrifugal distortion constants other than Φ_{JK} resulted in no improvement of the fit. It was therefore decided to exclude most of these lines from the fit. The Watson Hamiltonian is therefore obviously insufficient for several of these low- K_{-1} lines. Attempts were consequently made to fit the $K_{-1} \leq 2$ lines to the more advanced Hamiltonian used by Nielsen, employing his computer program Asmix,⁴⁵ but no significant improvements were seen using this approach.

The c -type lines with $K_{-1} \geq 3$ should coalesce with the corresponding b -type lines, because sc is almost a prolate rotor in the case of no tunneling, and should be split by $\pm\Delta$ from these frequencies in the case of tunneling. No such splittings were observed and no obvious broadening of lines was seen. It is therefore concluded that the tunneling frequency in fact is exceptionally small in this case and definitely less than the resolution of our spectrometer (0.5 MHz). The estimate of $\Delta = 15$ MHz made from the model discussed above must be too large.

Comparison of the rotational and centrifugal distortion constants of the ground vibrational state and the theoretical constants (Table 2) reveals that the MP2 constants are in very good agreement with the experimental counterparts, and good agreement is seen for the B3LYP constants.

Vibrationally Excited States. The ground state transitions were accompanied by several series of satellite lines presumably belonging to vibrationally excited states. Three excited states

belonging to three different normal modes were assigned in a manner similar to the one described for the ground vibrational state. The spectra are listed in the Supporting Information, Tables 2S–4S, and the spectroscopic constants are displayed in Table 4. The vibration–rotation constants (the α 's) appearing in Table 5 have been derived from $\alpha = X_0 - X_1$,²⁷ where X_0 is the rotational constants of the ground vibrational state and X_1 is the corresponding rotational constant of the first excited state. Their B3LYP/aug-cc-pVTZ counterparts have also been listed in this table.

The strongest satellite spectrum has roughly 65% of the intensity of the ground vibrational state at room temperature. Relative intensity measurements performed as described elsewhere⁴⁶ yielded a vibrational frequency of 77(20) cm^{-1} for this normal mode. This satellite is assumed to be the first excited state of the torsion about the C2–C3 bond. The harmonic B3LYP vibrational frequency of this mode is 95 cm^{-1} (Table 6s; Supporting Information). It is seen from Table 5 that there is good agreement between the B3LYP vibration–rotation constants (the α 's) and their experimental counterparts, which supports this assignment.

The intensity of the second lowest excited state is roughly 50% of the intensity of the ground state at room temperature. Relative intensity measurements yielded 152(25) cm^{-1} for this mode, which is assumed to be the first excited state of the lowest bending vibration, whose harmonic B3LYP frequency is 182 cm^{-1} . The experimental and theoretical α 's show only an order-of-magnitude agreement in this case (Table 5).

Finally, the first excited state of the C–S torsion were assigned and found to have a frequency of 165(30) cm^{-1} by relative intensity measurements, compared to 219 cm^{-1} found in the B3LYP calculations. The comments made for the α 's in the previous section for the lowest bending vibration apply in this case too. Interestingly, no indication of splittings due to tunneling was observed for this excited state, which would be expected to have a significantly larger splitting than that of the ground vibrational state.

The next three fundamentals are calculated to occur at 350, 356, and 523 cm^{-1} (not given in Tables 1 or 2) but none of the corresponding excited state MW spectra were assigned, presumably because of insufficient intensities.

CF₃CH₂SD Species. The MP2 structure was used to predict the rotational constants of this species. The assignment of its MW spectrum, which is listed in Table 5S in the Supporting Information, was straightforward and the spectroscopic constants obtained from 202 transitions are listed in Table 3. Kraitchman's equations⁴⁷ were employed to calculate the substitution coordinates⁴⁸ of the H atom of the thiol group as $a = |193.7(16)|$, $b = |86.8(36)|$, and $c = |197.0(32)|$ pm, where the uncertainties have been calculated as recommended by van Eijck.⁴⁹ The MP2 structure (Table 2) yields $a = |203.0|$, $b = |179.9|$, $c = |181.6|$ pm, respectively, for these coordinates. The agreement is not perfect but allows one to conclude that the H7–S1–C2–C3 dihedral angle must be close to the theoretical values of 70.2° (B3LYP; Table 1) and 68.5° (MP2). A value of 68(5)° with a liberal uncertainty limit of $\pm 5^\circ$ is estimated for this dihedral angle by varying the H7–S1–C2–C3 dihedral angle in a systematic manner, keeping the rest of the MP2 structure fixed. The corresponding angle in CH₃CH₂SH is 61.75(97)°.³⁰

Discussion

There is no indication in the MW spectrum of the existence of a second form (i.e., *ap*), which is in agreement with the B3LYP prediction (see above). This behavior of CF₃CH₂SH

contrasts with that of CH₃CH₂SH, where both a H–S–C–C *synclinal* and an *antiperiplanar* form have been identified with the *synclinal* rotamer more stable than the *antiperiplanar* conformer by 1.69(18) kJ/mol.⁵⁰

The conformational properties of CF₃CH₂SH are presumably controlled by a variety of intramolecular forces. Internal H bonding may presumably explain why the H–S–C–C *synclinal* conformer is more stable in CF₃CH₂SH than in CH₃CH₂SH. From the MP2 structure in Table 1, it is calculated that the internal H bond in CF₃CH₂SH is characterized by a nonbonded H7···F4 distance of 271 pm, compared to the sum, 255 pm, of the van der Waals radii⁵¹ of hydrogen (120 pm) and fluorine (135 pm). The nonbonded S–H···F angle is 94.7°, far from the ideal linear configuration (180°). Interestingly, the C3–F4 bond and S1–H7 bonds are 7.0° from being parallel. The fluorine atom forms the negative end of the C3–F4 bond moment,⁵² whereas the sulfur atom forms the negative end of the S1–H7 bond moment.⁵² The C3–F4 and S1–H7 bond moments are therefore almost *antiparallel*, which results in an ideal electrostatic stabilizing effect.

The *ap* conformer of CF₃CH₂SH is a first-order transition state according to the B3LYP calculations above, whereas the corresponding rotamer of CH₃CH₂SH represents a minimum on its potential energy hypersurface. The reason for this difference is not clear, but it is possible that the lone-pair electrons of the sulfur atom in *ap* are repelled by the strongly electronegative fluorine atoms, resulting in a destabilization of this rotamer. A similar repulsion is absent in the “stable” *antiperiplanar* form of CH₃CH₂SH.

Acknowledgment. We thank Anne Horn for her skillful assistance. The Research Council of Norway (Program for Supercomputing) is thanked for a grant of computer time.

Supporting Information Available: Spectra of the ground and vibrationally excited of the parent species, and the spectrum of the ground state of the SD species. This material is available free of charge via the Internet at <http://pubs.acs.org>.

References and Notes

- (1) Møllendal, H.; Mokso, R.; Guillemin, J.-C. *J. Phys. Chem. AA* 2008, 112, 3053 and references therein.
- (2) Scappini, F.; Favero, P. G.; Cervellati, R. *Chem. Phys. Lett.* **1975**, 33, 499.
- (3) Bolton, K.; Sheridan, J. *Spectrochim. Acta A* **1970**, 26, 1001.
- (4) Bhaumik, A.; Brooks, W. V. F.; Dass, S. C.; Sastry, K. V.; L, N. *Can. J. Chem.* **1970**, 48, 2949.
- (5) Marstokk, K.-M.; Møllendal, H. *Acta Chem. Scand., Ser. A* **1983**, A37, 477.
- (6) Marstokk, K.-M.; Møllendal, H. *Acta Chem. Scand., Ser. A* **1986**, A40, 402.
- (7) Marstokk, K.-M.; Møllendal, H. *NATO ASI Ser., Ser. C* **1987**, 212, 57.
- (8) Cole, G. C.; Møllendal, H.; Guillemin, J.-C. *J. Phys. Chem. A* **2006**, 110, 9370.
- (9) Cole, G. C.; Møllendal, H.; Khater, B.; Guillemin, J.-C. *J. Phys. Chem. A* **2007**, 111, 1259.
- (10) Marstokk, K.-M.; Møllendal, H. *Acta Chem. Scand.* **1994**, 48, 298.
- (11) Walsh, A. D. *Trans. Faraday Soc.* **1949**, 45, 179.
- (12) Marstokk, K.-M.; Møllendal, H. *Acta Chem. Scand.* **1991**, 45, 354.
- (13) Marstokk, K.-M.; Møllendal, H.; Stenstrøm, Y. *Acta Chem. Scand.* **1994**, 48, 711.
- (14) Fantoni, A. C.; Caminati, W. *J. Mol. Spectrosc.* **1990**, 143, 389.
- (15) Barkowski, S. L.; Hedberg, K. *J. Am. Chem. Soc.* **1987**, 109, 6989.
- (16) Nandi, R. N.; Boland, M. F.; Harmony, M. D. *J. Mol. Spectrosc.* **1982**, 92, 419.
- (17) Caminati, W.; Velino, B.; Schäfer, L.; Ewbank, J. D.; Siam, K. J. *Mol. Struct.* **1989**, 197, 123.
- (18) Marstokk, K.-M.; Møllendal, H. *Acta Chem. Scand.* **1997**, 51, 653.
- (19) Møllendal, H.; Leonov, A.; de Meijere, A. *J. Phys. Chem. A* **2005**, 109, 6344.

- (20) Møllendal, H.; Cole, G. C.; Guillemin, J.-C. *J. Phys. Chem. A* **2006**, *110*, 921.
- (21) Frisch, M. J.; Trucks, G. W.; Schlegel, H. B.; Scuseria, G. E.; Robb, M. A.; Cheeseman, J. R.; Montgomery, J. A., Jr.; Vreven, T.; Kudin, K. N.; Burant, J. C.; Millam, J. M.; Iyengar, S. S.; Tomasi, J.; Barone, V.; Mennucci, B.; Cossi, M.; Scalmani, G.; Rega, N.; Petersson, G. A.; Nakatsuji, H.; Hada, M.; Ehara, M.; Toyota, K.; Fukuda, R.; Hasegawa, J.; Ishida, M.; Nakajima, T.; Honda, Y.; Kitao, O.; Nakai, H.; Klene, M.; Li, X.; Knox, J. E.; Hratchian, H. P.; Cross, J. B.; Adamo, C.; Jaramillo, J.; Gomperts, R.; Stratmann, R. E.; Yazyev, O.; Austin, A. J.; Cammi, R.; Pomelli, C.; Ochterski, J. W.; Ayala, P. Y.; Morokuma, K.; Voth, G. A.; Salvador, P.; Dannenberg, J. J.; Zakrzewski, V. G.; Dapprich, S.; Daniels, A. D.; Strain, M. C.; Farkas, O.; Malick, D. K.; Rabuck, A. D.; Raghavachari, K.; Foresman, J. B.; Ortiz, J. V.; Cui, Q.; Baboul, A. G.; Clifford, S.; Cioslowski, J.; Stefanov, B. B.; Liu, G.; Liashenko, A.; Piskorz, P.; Komaromi, I.; Martin, R. L.; Fox, D. J.; Keith, T.; Al-Laham, M. A.; Peng, C. Y.; Nanayakkara, A.; Challacombe, M.; Gill, P. M. W.; Johnson, B.; Chen, W.; Wong, M. W.; Gonzalez, C.; Pople, J. A. *Gaussian 03*, revision B.03; Gaussian, Inc.: Pittsburgh, PA, 2003.
- (22) Møller, C.; Plesset, M. S. *Phys. Rev.* **1934**, *46*, 618.
- (23) Becke, A. D. *Phys. Rev. A* **1988**, *38*, 3098.
- (24) Lee, C.; Yang, W.; Parr, R. G. *Phys. Rev. B* **1988**, *37*, 785.
- (25) Dunning, T. H., Jr. *J. Chem. Phys.* **1989**, *90*, 1007.
- (26) Watson, J. K. G. *Vibrational Spectra and Structure*; Elsevier: Amsterdam, 1977; p 6.
- (27) Gordy, W.; Cook, R. L. *Techniques of Chemistry, Vol. XVII: Microwave Molecular Spectra*; John Wiley & Sons: New York, 1984; Vol. XVII.
- (28) Kojima, T.; Nishikawa, T. *J. Phys. Soc. Jpn.* **1957**, *12*, 680.
- (29) Hayashi, M.; Imaishi, H.; Kuwada, K. *Bull. Chem. Soc. Jpn.* **1974**, *47*, 2382.
- (30) Nakagawa, J.; Kuwada, K.; Hayashi, M. *Bull. Chem. Soc. Jpn.* **1976**, *49*, 3420.
- (31) Beagley, B.; Jones, M. O.; Zanjanchi, M. A. *J. Mol. Struct.* **1979**, *56*, 215.
- (32) Ray, B. S. *Z. Phys.* **1932**, *78*, 74.
- (33) Lewis, J. D.; Malloy, T. B., Jr.; Chao, T. H.; Laane, J. *J. Mol. Struct.* **1972**, *12*, 427.
- (34) Bjørseth, A. Personal communication, 1974.
- (35) Pitzer, K. S.; Gwinn, W. D. *J. Chem. Phys.* **1942**, *10*, 428.
- (36) Xu, L.-H.; Fraser, G. T.; Lovas, F. J.; Suenram, R. D.; Gillies, C. W.; Warner, H. E.; Gillies, J. Z. *J. Chem. Phys.* **1995**, *103*, 9541.
- (37) Hirota, E. *J. Mol. Spectrosc.* **1968**, *26*, 335.
- (38) Mirri, A. M.; Scappini, F.; Cervellati, R.; Favero, P. G. *J. Mol. Spectrosc.* **1976**, *63*, 509.
- (39) Kakar, R. K.; Quade, C. R. *J. Chem. Phys.* **1980**, *72*, 4300.
- (40) Hirota, E. *J. Phys. Chem.* **1979**, *83*, 1457.
- (41) Griffiths, J. H.; Boggs, J. E. *J. Mol. Spectrosc.* **1975**, *56*, 257.
- (42) Mokso, R.; Møllendal, H.; Guillemin, J.-C. *J. Phys. Chem. A* **2008**, *112*, 4601.
- (43) Macdonald, J. N.; Norbury, D.; Sheridan, J. *J. Chem. Soc., Faraday Trans.* **1978**, *74*, 1365.
- (44) Sørensen, G. O. *J. Mol. Spectrosc.* **1967**, *22*, 325.
- (45) Nielsen, C. J. *Acta Chem. Scand., Ser. A* **1977**, *A31*, 791.
- (46) Esbitt, A. S.; Wilson, E. B. *Rev. Sci. Instrum.* **1963**, *34*, 901.
- (47) Kraitchman, J. *Am. J. Phys.* **1953**, *21*, 17.
- (48) Costain, C. C. *J. Chem. Phys.* **1958**, *29*, 864.
- (49) Van Eijck, B. P. *J. Mol. Spectrosc.* **1982**, *91*, 348.
- (50) Schmidt, R. E.; Quade, C. R. *J. Chem. Phys.* **1975**, *62*, 3864.
- (51) Pauling, L. *The Nature of the Chemical Bond*; Cornell University Press: Ithaca, NY, 1960.
- (52) Smyth, C. P. *Dielectric Behavior and Structure*; McGraw-Hill: New York, 1955.

JP803481K